Available online at www.sciencedirect.com

ScienceDirect

Procedia CIRP 93 (2020) 1520–1525

www.elsevier.com/locate/procedia

53rd CIRP Conference on Manufacturing Systems

Grinding wheel wear and material removal mechanisms during grinding of polycrystalline diamond

T. Bergs[a], U. Müller[a]*, F. Vits[b], S. Barth[a]

[a]*Laboratory for Machine Tools and Production Engineering (WZL) of RWTH Aachen University, Campus-Boulevard 30, 52074 Aachen, Germany*

[b]*Gehring Technologies GmbH, Gehringstraße 28, 73760 Ostfildern, Germany*

* Corresponding author. Tel.: +49-241-80-28188; fax: +49-241-80-22293. *E-mail address:* u.mueller@wzl.rwth-aachen.de

Abstract

Grinding is a widely used technology in the manufacturing process of polycrystalline diamond (PCD) cutting tools. Due to the high hardness of PCD, the process efficiency of grinding is low. In order to improve the process efficiency, an increased understanding of the interactions between the grinding wheel and the PCD workpiece has to be gained. Therefore, the subsurface material behavior during grinding of different PCD specifications was conducted in this article. To attain this, a screening of process input parameters was done to identify the thermal and mechanical load during grinding. The PCD workpieces ground by the preidentified parameters were then analyzed using transmission electron microscopy (TEM) to examine the subsurface material behavior. Based on the results of the TEM analysis, explanatory models for the material removal mechanisms and the grinding wheel wear were developed.

Keywords: Polycrystalline Diamond, Grinding Wheel Wear, Material Removal Mechanisms

1. Introduction

The global cutting tool market is facing increasing demands on both economic and ecologic sustainability [1]. Cutting tool materials like polycrystalline diamond (PCD) are in great demand, which is driven by an increased application of advanced materials, e.g. fiber-reinforced composites, in the aerospace industry [2]. According to Airbus [3], more than 38,000 new aircraft will be produced until year 2038 and thus PCD cutting tool market is growing.

Due to superior cutting performance of PCD compared to other cutting tool materials when drilling, milling and turning non-ferrous materials [4], PCD shows the highest annual growth rates in the cutting material market [5]. The technology chain for manufacturing PCD cutting tools primarily consists of eroding, grinding and laser processing. Grinding still outperforms other manufacturing processes when a high quality surface integrity is needed [6], particular in machining superhard materials.

Despite the grinding process of PCD is well established, grinding of PCD is characterized by low material removal rates and high grinding wheel wear. A reduction of the grinding wheel wear decreases the amount of synthetic diamond used as abrasive grains in grinding wheels. Since the synthesis of diamond is going along with high energy consumption, an increased process efficiency of the grinding process decreases the environmental impact of a PCD cutting tool life cycle [7]. In order to increase the process efficiency, further research on the interactions between the grinding wheel and the workpiece subsurface during grinding PCD has to be done.

2. State of research

Schindler observed different material removal mechanisms during grinding of PCD (CTB010, Element Six) depending on

10.1016/j.procir.2020.03.083

the mechanical process load [8]. According to Schindler, the grinding process can be split into grinding with mechanical overload and without mechanical overload of the diamond grains in the PCD. In addition to a mechanically induced crack formation, Schindler et al. identified thermophyscial phase transitions from diamond to graphite during grinding [9]. They also found, that chemical reactions between carbon and oxygen occur, which support the graphitization of diamonds [10].

Vits et al. conducted friction tests according to the pin-on-disk principle. While running the friction tests, they measured the forces and the temperatures in the contact zone between samples made from monocrystalline diamond and a rotating PCD blank [11]. For normal forces and relative velocities, as they occur in PCD grinding, Vits et al. identified maximum temperatures around $T \approx 370$ °C for single grain contact. However, these temperatures are not sufficient to cause thermophysical transformation reactions in diamond. Hence, they concluded that the temperatures in the contact zone during PCD grinding must be lower than previously assumed, and the material removal mechanisms are primarily mechanically driven.

A transfer of the findings of Vits et al. to a multigrain contact was not conducted so far. Furthermore, an analysis of the subsurface of ground PCD workpieces with different grain sizes and amount of cobalt has not yet been carried out. Therefore, this article contributes to identifying subsurface material behavior, e.g. crack propagation, of PCD during grinding considering varying PCD specifications. Hence, a screening of the grinding process parameters to identify the mechanical and thermal load during grinding was done first. Subsequently, the material removal mechanisms were explained based on the analysis of TEM images of the subsurface of the ground PCD workpieces and the identified mechanical and thermal load.

3. Experimental Setup and Design of Experiments

The grinding tests were carried out on a S22p turbo tool grinding machine from ISOG Technology GmbH & Co. KG. Analogous workpieces from the manufacturer Element Six were used. The geometry of the analogous workpiece was adapted to the geometry of a cutting insert of a standard PCD indexable insert (Figure 1, (a)). The total thickness $b_{tot} = 1.6$ mm of the analogous workpiece was subdivided into the thickness of a cemented carbide substrate $b_{WC} = 1$ mm and the thickness of a PCD layer $b_{PCD} = 0.6$ mm. The width of the analogous workpiece was $d_{PCD} = 4$ mm and the total height was $h_{PCD} = 15$ mm. A stock removal $z_{tot} = 0.2$ mm was machined at every test point. This resulted in the PCD machining volume $V_{PCD} = 0.48$ mm³.

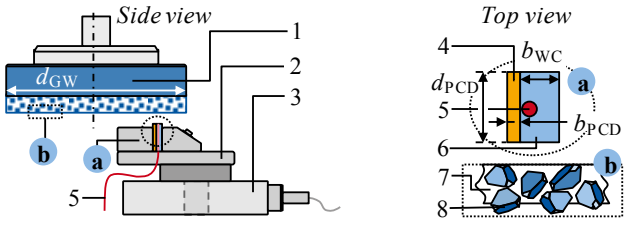

1: Grinding wheel
2: Vice
3: Force dynamometer
4: PCD / Analogous workpiece
5: Pyrometer fiber
6: Cemented carbide
7: Ceramic bond
8: Diamond grain

Fig. 1. Experimental Setup of the grinding tests

An borehole of diameter $d_b = 800$ µm was eroded into the carbide substrate of the analogous workpieces. The glass fiber of a type 3MH2 pyrometer from Optris GmbH was inserted in the borehole, which was machined during the grinding process. The measuring spot of the pyrometer was aligned with the grinding layer to enable the measurement of the temperature of the grinding wheel surface. Grinding tests with three different PCD specifications (CTB010, CTM302, CMX850) provided by the manufacturer Element Six were conducted. The PCD specifications were varying regarding the diamond grain size and the amount of cobalt (Table 1).

Table 1. Material properties of different PCD specifications

Specific value	Unit	PCD CTB010	PCD CTM302	PCD CMX850
Average diamond size d_k	µm	10	2 & 30	0.5–1
Cobalt amount x_{co}	Ma.-%	10–13	10–13	> 15

The analogous workpieces were clamped in a vice (Figure 1). To ensure sufficient rigidity of the set-up the cantilever length of the workpiece from the vice was $h_c < 1$ mm. The vice was mounted on a multi-component force dynamometer type 9119AA2 from Kistler Instrumente AG, which measured the grinding force components in three orthogonal spatial directions (Figure 1). The grinding process was carried out using surface-side longitudinal grinding kinematics. Before each stroke, the grinding wheel was infed relative to the analogous workpiece by the amount a_e. After the grinding stroke, the grinding wheel was lifted vertically and returned to its initial position. Further infeeds were conducted at the inner radius of the grinding wheel, followed by grinding strokes until the stock removal $z_{tot} = 0.2$ mm was machined. A ceramic bonded diamond grinding wheel from Tyrolit Schleifmittelwerke Swarovski KG with the specification 6A2H D15-VB+ Skytec-PCD-Basic+ was used. The diameter of the grinding wheel was $d_{GW} = 150$ mm and the width of the grinding layer was $b_{GW} = 20$ mm.

Before each test, the grinding wheel was dressed rotary with a corundum dressing wheel from Tyrolit Schleifmittelwerke Swarovski KG with the specification 89A400H5AV83. The dressing speed ratio was $q_d = -0.6$, the dressing depth of cut per stroke was $a_{ed,i} = 5$ µm and the dressing feed rate was $v_{fad} = 500$ mm/min. In order to cover the initial grinding wheel wear, a stock removal of $z_{tot} = 0.2$ mm of the analogous workpiece was ground after each dressing cycle.

The screening of grinding parameters was carried out according to a partial factorial design of experiments during grinding of the PCD specification CMX850 (Figure 2). The process input parameters grinding wheel circumferential speed v_{GW}, depth of cut per stroke $a_{e,i}$ and feed rate v_f were varied in the listed factor stages. During grinding, the process state parameters grinding normal force F_n, grinding tangential force F_t and process temperature T_p were measured to identify the highest respectively lowest mechanical and thermal load. The identified test points were then conducted for each aforementioned PCD specification (Table 1).

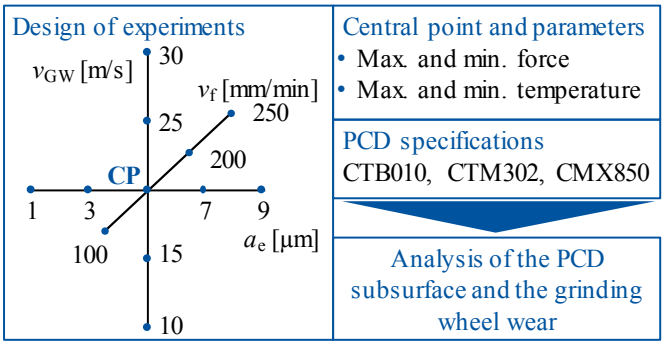

Fig. 2. Design of experiments for the grinding tests

4. Results

Transmission electron microscope (TEM) images of the PCD workpiece subsurface were taken. For this purpose, lamellae were separated from the ground PCD workpiece using the focused ion beam (FIB) method. During grinding PCD CMX850, the maximum and minimum thermal (T_{max} = 169 °C, T_{min} = 88 °C) and the maximum and minimum mechanical loads ($F_{n,max}$ = 158 N, $F_{n,min}$ = 91 N) were measured to enable a qualitative analysis of the material removal mechanisms in PCD grinding.

Figure 3 shows a TEM image of an unground PCD CMX850 sample made for reference in order to enable an evaluation of the influence of the thermal and mechanical loads during the grinding process on the PCD subsurface. The unground PCD structure consisted of individual, randomly oriented diamond crystals. These were fused together at their grain boundaries in the sintering process. Dislocation lines along the crystal planes could be observed both within the cobalt crystals and within the diamond crystals (Figure 3). Furthermore, the diamond crystals showed localized signs of internal stress. This state of PCD after a high-pressure liquid-phase sintering process was also described by Wamsley et al. [12]. Therefore, the internal stress of the diamond crystals can be referred to the high pressures of up to p = 6 GPa during sintering. High pressures in the contact points between the individual diamonds led to the partial fracture of the diamond crystals and to a conversion of the diamond into graphite. The cobalt infiltrated the gaps between the diamonds. The graphite disintegrated in the cobalt due to the thermodynamic boundary conditions [12].

In the following, only the test points showing the highest normal force $F_{n,max}$ for each PCD specification are presented, since the influence of the temperature on the modification of the workpiece subsurface was found minor compared to the normal force.

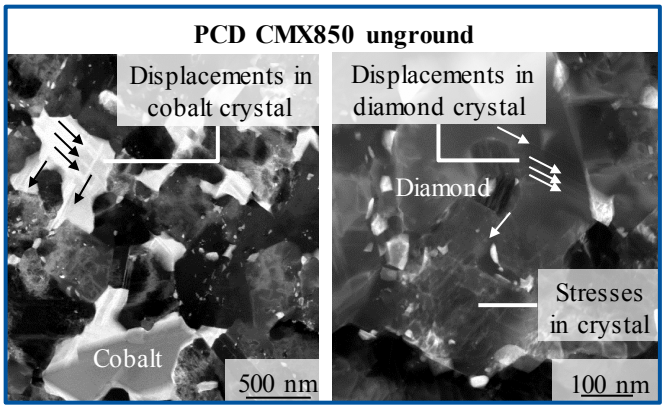

Fig. 3. TEM image of an unground PCD CMX850 sample

Figure 4 shows the TEM image of the subsurface of the PCD CMX850 workpiece, which was ground with a high depth of cut per stroke of a_e = 9 µm. The highest grinding force ($F_{n,max}$ = 158 N) was measured during grinding of this workpiece. The subsurface showed no signs of a thermally induced conversion of diamond to graphite due to the process temperature T in the contact zone. This observation supports the hypothesis of Vits et al. that the process temperatures in PCD grinding under common conditions are below the conversion temperature for diamond [11].

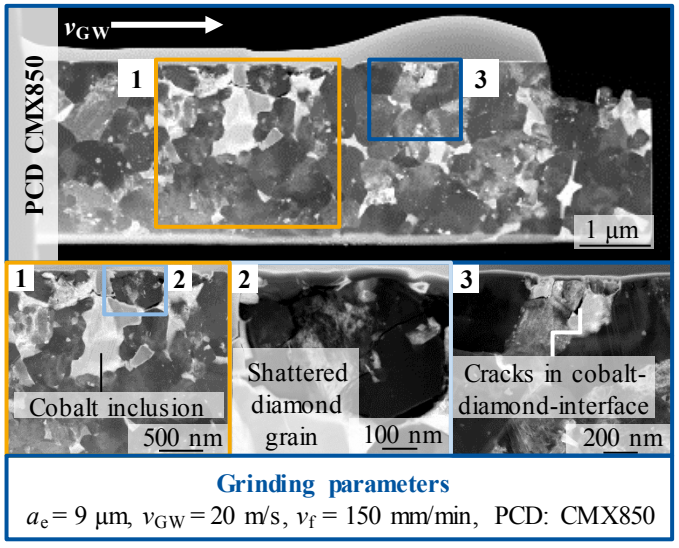

Fig. 4. Influence of a high depth of cut a_e on the subsurface of PCD CMX850 (cobalt-diamond interface)

However, a mechanical influence on the PCD subsurface was visible. Characteristics of brittle material removal could be seen particularly in the area of cobalt inclusions (Figure 4, magnification 1). Transcrystalline cracks were formed in the monocrystalline diamonds (Figure 4, magnification 2). Intercrystalline cracks also occurred at the grain boundary between the cobalt and monocrystalline diamond grain (Figure 4, magnification 3). The maximum depth of damage in the form of cracks was $t_{g,max}$ = 500 nm. Almost no damage due to cracks could be observed in the areas near the surface, where no cobalt was present. The material removal in these areas was most

likely due to microabrasion during the overrun of an abrasive grain. In areas with localized, near-surface cobalt inclusions, the microstructure was weakened due to the comparatively low Young's modulus of cobalt (E_{co} = 211 GPa, E_{dia} = 1000 GPa). In these areas, the grinding force caused the cobalt to deform elastically in a wider range than the diamond. The resulting shear stresses in the grain boundary between cobalt and diamond could be an explanation for the intercrystalline cracks. Another explanation for the intercrystalline cracking could be the highly different coefficients of thermal expansion of cobalt and diamond. These differ by a factor f of $4.5 \leq f \leq 8$, so that internal stresses can occur in the heating of the PCD structure during the grinding process, which can exceed the cohesion of the covalent bonds [13]. In addition, cobalt inclusions in surface near areas located below two directly connected diamond grains caused a kind of "eggshell effect". This effect resulted in transcrystalline cracks in the diamond. The growth of intercrystalline and transcrystalline cracks led to a breakout of diamond grains and diamond fragments and thus to material loss. Signs of ductile deformation of the PCD microstructure, due to the process loads during grinding, were not observed.

For the grinding of PCD CTB010, the same material removal mechanisms were observed as for grinding of PCD CMX850 (Figure 5). Large diamond grains or fused diamond grains without direct contact to near-surface cobalt were machined abrasively.

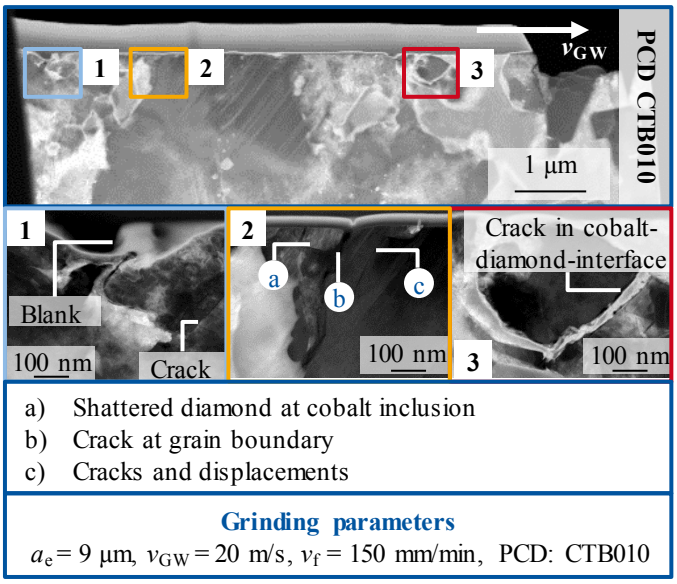

Fig. 5. Subsurface of a sample made of PCD CTB010 ground with a high depth of cut a_e

Where near-surface cobalt inclusions occur, material removal in the form of transcrystalline (Figure 5, magnification 2) and intergranular (Figure 5, magnification 3) crack formation dominated. Furthermore, blanks could be observed on the surface, which indicated a breakout of diamond grains from the PCD composite (Figure 5, magnification 1). In the grinding direction, diamond grains located behind these blanks showed an increased amount of cracks, dislocations and signs of internal stresses (Figure 6, magnification 2). A possible explanation for this could be localized force peaks when an abrasive grain collides with the flank of the diamond grain in the PCD. The maximum depth of damage due to cracking was $t_{g,max}$ = 500 nm and was therefore on the same level with the maximum depth of damage $t_{g,max}$ during grinding PCD CMX850 with identical grinding parameters.

Figure 6 shows the TEM image of the subsurface of a PCD CTM302 workpiece ground with a high depth of cut per stroke of a_e = 9 µm. Intercrystalline (Figure 6, magnification 3) and transcrystalline (Figure 6, magnifications 1 and 2) cracks also occurred during grinding of PCD CTM302 in areas with near-surface cobalt. Diamonds in areas without near-surface cobalt were abrasively machined. Diamonds which lay behind localized defects in the PCD surface in the grinding direction (Figure 6, magnification 1) showed cracks and displacements. The PCD specification had no influence on the maximum depth of damage due to crack formation, which amounted to $t_{g,max}$ = 500 nm.

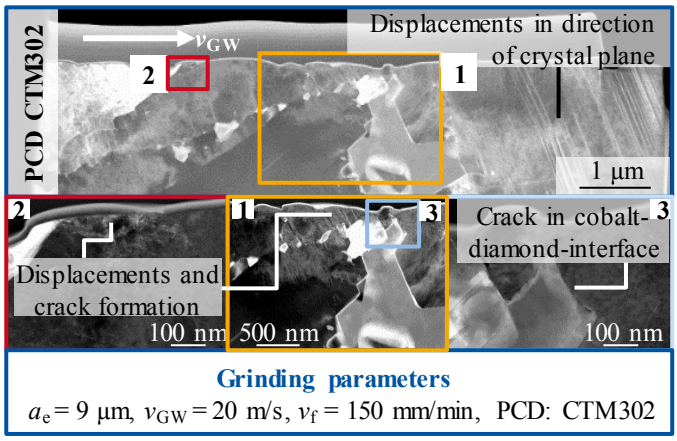

Fig. 6. Subsurface of a PCD CTM302 sample ground with a high depth of cut a_e

5. Discussion

In the previous section, the material removal mechanisms for PCD grinding were identified using TEM images. The identified material removal mechanisms were summarized in an explanatory model in Figure 7.

The material removal mechanisms were strongly dependent on the occurrence of near-surface cobalt inclusions. In areas where no cobalt inclusions were present, the PCD structure was highly resistant to cracking and breakout of diamond grains. The machining of the diamonds was based on abrasive material removal. This hypothesis was also presented by Kenter based on the investigation of ground PCD surfaces [15]. Cracks in the diamond crystal could only be identified sporadically. There were no signs of plastic deformation in the PCD structure. A thermally induced conversion of diamond into graphite or combustion of diamond could be excluded on the basis of the investigations, since TEM images did not show any signs of graphite formation due to the grinding process. Based on this observation, the thesis of Schindler et al. regarding thermophysical effects in PCD grinding tend to favor process efficiency must be limited for the parameter space [9].

Brittle material removal dominated in areas where near-surface cobalt inclusions were present. Transcrystalline cracks in diamond grains and intercrystalline cracks in the interface between cobalt and diamond grains were predominant. These phenomena were attributed to the very different Young's moduli and coefficients of thermal expansion of cobalt and diamond. The high surface pressures during grinding led to an elastic deformation of the subsurface. The elastic strain on the diamonds and the cobalt resulted in shear stresses in the cobalt-diamond interface and finally led to intercrystalline cracks. In addition, shear stresses were induced by the highly differing expansion of the diamonds and cobalt as a result of the process heat. This phenomenon was also observed by Neises [13]. Transcrystalline cracks also occurred in the diamond grains. These cracks were attributed to the diamond crystals exceeding the tensile strength due to the alternating thermal and mechanical stresses induced by the grinding process. As a result of crack growth, pieces of individual diamond grains or complete diamond grains broke out of the composite and left blanks in the PCD surface.

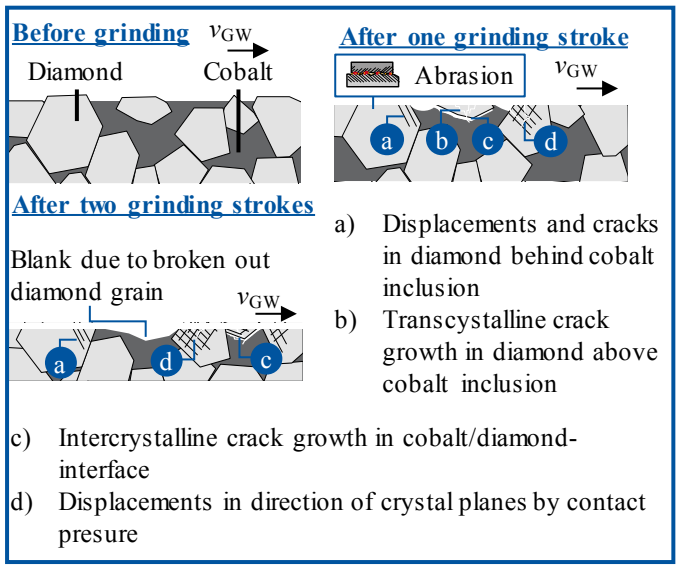

Fig. 7. Explanatory model for the material removal mechanisms in PCD-grinding

In the grinding direction, diamond grains located behind these blanks showed an increased amount of cracks, dislocations and signs of internal stresses. This was an indication of localized force peaks occurring when an abrasive grain collided with the flanks of these diamonds in the PCD. The size of the blanks depended on the grain size of the respective PCD specification and the load spectrum. When a mechanical load limit was exceeded, a higher amount of integral diamond grains broke out of the PCD structure. The size of the resulting blanks correlated with the grain size of the diamond grains in the PCD composite. Below this mechanical load limit, the diamond skeleton had sufficient resistance to grain breakout, and abrasive material removal dominated. In areas where near surface cobalt inclusions occurred and a diamond grain was still fused with directly adjacent diamond grains, an "eggshell effect" was assumed. Here, the structurally weakened diamond grain was retained by the adjacent diamond grains, and the high contact pressures in the grinding process caused the cobalt to deform elastically beneath the diamond. This led to the formation of transcrystalline and intercrystalline cracks and the breakout of diamond particles or complete diamond grains.

The properties of the subsurface of the PCD workpieces after grinding were used to explain the interaction between the surfaces of the grinding wheel and the PCD workpiece and, in turn, the grinding wheel wear mechanisms. These were summarized in an explanatory model in Figure 8.

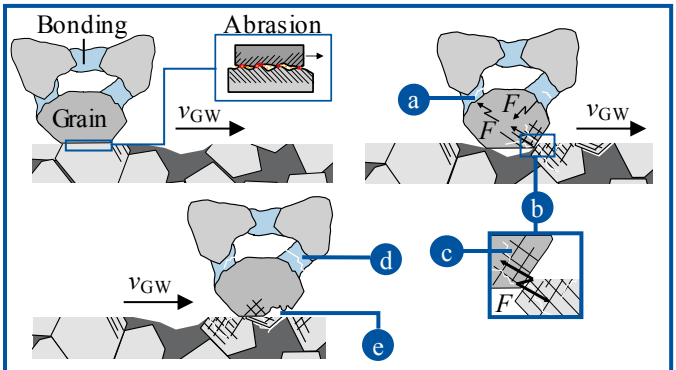

Fig. 8. Explanatory model for grinding wheel wear mechanisms during PCD grinding

In previous work, Vits et al. identified the abrasive wear of abrasive grains, partial grain fracture and grain breakout as a result of bonding fracture as the causes for the wear of ceramic bonded diamond grinding wheels during PCD grinding [14]. These grinding wheel wear mechanisms were also observed by Kenter [15]. Based on the analysis of the PCD subsurface, abrasive grains were in contact with areas of the workpiece in which intergrown diamonds were present. This resulted in abrasive grinding wheel wear and led to a flattening of the abrasive grains. In areas of the workpiece surface where blanks or comparatively soft cobalt inclusions occurred, it can be assumed that the grinding layer is elastically compressed due to the contact force. This is followed by a local decompression of the grinding layer due to a momentary decrease of the contact force. The result of the decompression are individual diamond abrasive grains indented completely or partially into the blanks or into the elastically yielding cobalt during the overrun. The amount of elastic expansion was added to the kinematic chip thickness of the individual grains. The abrasive grains interlock to subsequent diamonds in the PCD composite. This resulted in local dynamic force peaks at the contact point between the diamond abrasive grain and the diamond grain in PCD. These force peaks partially exceeded the tensile strength of diamond and led to stresses, displacements, and transcrystalline cracks in the abrasive grains and diamonds in the PCD. This resulted in a partial fracture of the diamonds for

the two active partners. Furthermore, the force peaks caused the comparatively brittle bonding of the grinding layer to break, so that complete abrasive grains broke out of the grinding wheel bond.

The amplitude of the force peaks depended on the size of the blanks in the PCD surface. The size of the blanks in turn correlated with the grain size of the diamonds in the PCD composite. This could explain different grinding ratios when grinding different PCD specifications. High grinding wheel circumferential speeds also led to significantly higher grinding wheel wear. One can assume that this is due to an increase in the grain engagement frequency with increasing grinding wheel circumferential speed, which resulted in a disruption of the brittle ceramic bond. A thermally induced conversion of the diamond abrasive grains into graphite or a combustion of the diamond abrasive grains is unlikely. There were no signs of these phenomena in the external PCD zone. The temperatures in the grinding layer were assumed below the temperatures in the PCD edge zone due to the very short exposure time to process heat.

4. Conclusions

In this article, the subsurface material behavior of three different PCD specifications during grinding was discussed. Following conclusions can be drawn from this article:

- Polycrystalline diamond is both abrasively machined and locally shattered during grinding.
- The occurrence of near-surface cobalt inclusions favored brittle machining mechanisms.
- The quantity and distribution of cobalt in the PCD workpiece influences the proportion of abrasive and brittle machining during the grinding process.
- Grinding wheel wear is dominated by abrasion as long as the grains of the grinding wheel are in contact with areas of intergrown diamond grains of the PCD workpiece.
- The result of abrasive wear was a flattening of the grains in the grinding wheel.
- An increasing grain engagement frequency due to an increasing grinding wheel circumferential speed was identified as an essential driver for the mechanical disruption of the grinding wheel and thus for grinding wheel wear.

Acknowledgements

The authors thank the German Research Foundation for funding this work within the projects KL500/140-1 „Analyse der Zerspanungs- und Abtragsmechanismen beim Schleifen hochharter Schneidstoffe am Beispiel von polykristallinem Diamant“ and KL500/193-1 „Analyse der Verschleiß-mechanismen beim PKD-Schleifen mit keramisch gebundenen Diamantschleifscheiben auf Basis eines Reibungsmodells“.

References

[1] Li, B.; Cao, H.; Yan, J.; Jafar, S.: A life cycle approach to characterizing carbon efficiency of cutting tools. The International Journal of Advanced Manufacturing Technology, 93, 2017, p. 3347 – 3355
[2] Xu, J.; El Mansori, M.: Wear characteristics of polycrystalline diamond tools in orthogonal cutting of CFRP/Ti stacks. Science Arts & Métiers (SAM), Vol. 376 – 377, 2017, p. 91 – 106
[3] Airbus S.A.S.: Global Market Forecast. Cities, Airports & Aircraft, 2019
[4] M’Saoubi, R.; Axinte, D.; Soo, S. L.; Nobel, C.; Attia, H.; Kappmeyer, G.; Engin, S.; Sim, W.-M.: High performance cutting of advanced aerospace alloys and composite materials. CIRP Annals - Manufacturing Technology, 64, 2015, p. 557 – 580
[5] Bobzin, K.: High-performance coatings for cutting tools. Journal of Manufacturing Science and Technology, Vol. 18, 2017, p. 1 – 9
[6] Rahim, M. Z.; Li, G.; Ding, S.; Mo, J.: Electrical Discharge Grinding versus Abrasive Grinding in Polycrystalline Diamond Machining. Jurnal Teknologi (Sciences and Engineering), Vol. 74, No. 10, 2015, p. 79 – 87
[7] Gruenebaum, T.; Müller, U.; Rey, J.; Barth, S.; Bergs, T.: Life cycle oriented technology chain optimization: a methodology to identify the influences of tool manufacturing on environmental impacts caused in the tool’s use phase. Production Engineering, Vol. 13, 2019, p. 567 –577
[8] Schindler, F.: Zerspanungsmechanismen beim Schleifen von polykristal-linem Diamant. Dissertation RWTH Aachen, 2015
[9] Schindler, F.; Brocker, R.; Klocke, F.; Mattfeld, P.: A Discussion on Removal Mechanisms in Grinding Polycrystalline Diamond. Journal of Manufacturing Science and Engineering, Vol. 138, 011002, 2016
[10] Pastewka, L.; Moser, S.; Gumbsch, P.; Moseler, M.: Anisotropic Mechanical Amorphization Drives Wear in Diamond. Nature Materials, Vol. 10, 2010, p. 34 – 38
[11] Vits, F.; Trauth, D.; Mattfeld, P.; Klocke, F.; Vits, R.: Analysis of the Tribological Conditions in Grinding of Polycrystalline Diamond Based on Single Grain Friction Tests Using the Pin-Disk Principle. Key Engineering Materials 767, 2018, p. 259 – 267
[12] Walmsey, L. C.: Characteristics of diamond regrowth in a synthetic diamond compact. Journal of Material Science, Vol. 23, 1988, p. 1829
[13] Neises, A.: Einfluss von Aufbau und Eigenschaften hochharter nichtmetallischer Schneidstoffe auf Leistung und Verschleiß im Zerspanprozess mit geometrisch bestimmter Schneide. Forschungsbericht VDI, Vol. 2, Nr. 332, 1995
[14] Vits, F.; Trauth, D.; Mattfeld, P.; Klocke, F.: Schleifscheibenverschleiß bei der PKD-Bearbeitung. Wt Werkstattstechnik online, Jahrgang 108, Heft 6, 2018
[15] Kenter, M.: Schleifen von polykristallinem Diamant. Dissertation Universität Bremen, 1990